From Self-Affine to Logarithmic: Interfacial Fluctuation of a Stearic Acid Film upon Swelling in Water

Xiu-Hong Li, Ming Li,* and Zhen-Hong Mai

Institute of Physics, Chinese Academy of Sciences, Beijing 100080, P. R. China

Received: November 17, 2003; In Final Form: April 5, 2004

The interfacial structures of a solution-cast stearic acid film before and after immersion in water were studied by X-ray scattering combined with atomic force microscopy. It is shown that the interfaces of the as-deposited film are self-affine. After the film is immersed in water for a long time, water molecules penetrate into the hydrophilic interfaces, enlarging the distance between the adjacent bilayers. Theoretical fit indicates that the film takes on a liquid crystal character after being swollen by water. The interfaces in both cases are partially correlated and are well represented by the given correlation functions, except for a small discrepancy between the theory and the experiment on length scales shorter than 60 nm. The results help to provide a deeper insight into the interfaces of lipid multilayers during the intercalation of small molecules.

1. Introduction

Ordered, oriented organic/inorganic hybrid multilayered structures that possess fascinating optical or electronic properties can be prepared by immersing organic films in metallic salt solutions.[1−3] Details about the penetration of small molecules into the organic films are thus attracting attention of more chemists and material physicists. In the fabrication of the multilayered nanostructure of alternating polymers polystyrene-block-poly(4-vinylpyridine) (PS-b-P4vP) and gold nanoparticles, the thin polymer films were immersed into the ethanol solutions of HAuCl4 in order that the gold precursors can be coordinated to the pyridine units of the P4VP block.[1] Similarly, fatty acid Langmuir−Blodgett (LB) films were immersed in $MeCl_2$ (Me = Cu or Cd) aqueous solution and then reacted with H_2S gas to form fatty acid/MeS hybrid multilayered films.[2,3] At the same time, the effect of water on the structures of numerous phospholipid and fatty acid multilayers has been intensively studied.[4−9] Salditt et al. studied highly aligned phospholipid membranes in excess water by the X-ray specular and diffuse scattering techniques.[4,5] Vogel et al. investigated the temperature dependence of highly oriented multilamellar phospholipid membranes in excess water by X-ray reflectivity.[6] A discontinuous unbinding transition was exhibited from a substrate-bound, multilamellar state to a state of freely dispersed bilayers in water. Sharp et al. studied the surface morphology that arose when ultrathin supported films of poly(*d*,*l*-lactide) were immersed in water.[7] It showed that the films were initially flat with a root-mean-square (rms) roughness of approximately 2 nm, whereas after immersion the surfaces of the films were covered with craters. The craters had a narrow distribution of sizes and were typically micrometers in diameter. Marshbanks examined water transport in LB films of calcium stearate by attenuated total reflectance Fourier transform infrared spectroscopy.[8] The results indicated that the films absorbed at least 8 wt % (possibly up to 16 wt %) water when contacted with water. The effective diffusivity of water in the films was estimated to be in the range from about 10^{-13} to 10^{-10} cm^2/s. Girard et al. investigated the directional dependence of water penetration into arachidic acid LB films by a quartz crystal microbalance combined with surface forces apparatus.[9]

On the other hand, how the amphiphilic molecules undergo their transition from a solid phase to a lyotropic lamellar phase is regaining interest because of the potential application of the lyotropic liquid crystals in modern technology.[10,11] Historically, Lawrence studied the effect of water on a solid crystal of an amphiphilic substance.[12] It was suggested that water molecules penetrate the space between the polar heads of the adjacent bilayers, decreasing the Coulomb attraction between oppositely charged groups of polar heads. As the amount of water further increases, the polar heads of ionic lipids become ionized. The resulting loose packing makes it possible for the appearance of the lyotropic liquid crystalline phase. Recently, the process of water penetration and the emergence of a lyotropic lamellar phase in surfactant−water contact experiments have been visualized by cryo-transmission electron microscopy.[13] Despite the progress, the very detail of the solid to liquid crystal transition is still to be ascertained.

Information on the interfaces is crucial to understand the transition mentioned above. By monitoring the changes in interfacial fluctuations one can follow the structural transition induced by the intercalation of water molecules. This would help us have a comprehensive understanding of the process. X-ray scattering has proven to be one of the most powerful and direct methods to characterize the interfacial structures of the multilayers of amphiphilic molecules. Many groups have made remarkable contributions to this subject. Their results are summarized in several recent reviews.[14−17] The specular reflectivity detects the averaged structure in the direction perpendicular to the interfaces,[18] while the transverse diffuse scattering is sensitive to the lateral structure of the interfaces.[19] In this work, we report the X-ray scattering studies of a solution-cast stearic acid film before and after immersion in water. The specular reflectivity reveals a significant change in interlayer spacing, confirming that a large amount of water has penetrated into the interfaces. The transverse diffuse scattering shows that the water penetration results in a transition of the roughness scaling from the self-affine to the logarithmic type. The X-ray

* To whom correspondence should be addressed. Tel: +86-010-82649058. Fax: +86-010-82640224. Email: mingli@aphy.iphy.ac.cn.

10.1021/jp0375012 CCC: $27.50
Published on Web 05/20/2004

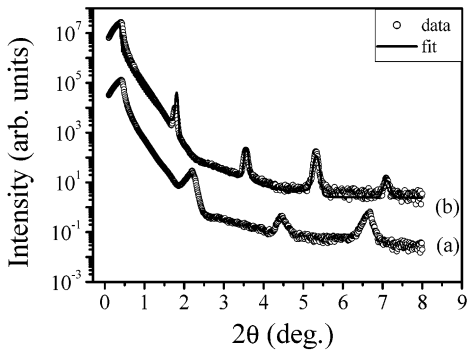

Figure 1. Specular reflectivity data and fit for the film: (a) before immersion; (b) after immersion.

observation was confirmed by atomic force microscopy (AFM) measurements.

2. Experimental Section

2.1. Chemicals. Stearic acid and 2-propanol are all analytical reagent grade and used as supplied. A Milli-Q water purification system (Millipore Corp.) was used to produce water with a resistivity of 1.8×10^5 Ω·m for all the experiments.

2.2. Sample Preparation. The stearic acid film was prepared on a hydrophilic Si(111) substrate. The silicon wafer was cleaned in a mixture of $H_2O/H_2O_2/H_2SO_4$ (5:1:1 by volume) at 90 °C for 20 min and then rinsed with water several times. After that they were cleaned again for approximately 20 min in a mixture of $H_2O/H_2O_2/NH_4OH$ (5:1:1 by volume) at 90 °C and then thoroughly rinsed with water until pH = 7. Following Seul and Sammon,[20] the stearic acid was dissolved in 2-propanol (2 mM) and pipetted onto the silicon substrate (10×10 mm^2), permitting the solution to spread spontaneously and the solvent to evaporate slowly. The evaporation rate of the solvent was controlled in a chamber over a period of 12 h before storing the sample in a desiccator for another 24 h. After the first cycle of measurements, the sample was immersed in water at 40 °C for more than 6 days. It can be estimated that the film contains about 50 bilayers according to the area per molecule, the total spread area, and the volume of the solution deposited.

2.3. X-ray Measurements. The X-ray measurements were performed on a Bruker D8-Advance diffractometer equipped with a Goebel mirror to obtain parallel X-ray beams and to suppress the Cu Kβ radiation. Cu Kα radiation was used. The incident beam was confined by a 0.1-mm slit 300 mm before the sample, and the scattered beam was confined by a 0.2-mm slit before the detector. The specular reflectivity measurement was performed by keeping the incidence angle θ_i equal to the exiting angle θ_f. The transverse diffuse scattering data were collected by rocking the sample, keeping the angle between the incidence and the reflection fixed. The detector is wide open in the out-of-plane direction to integrate effectively the scattering perpendicular to the scattering plane (along q_y).

2.4. Atomic Force Microscopy. The surface topography of the sample was observed with a NanoScope IIIa (DI Company, USA) atomic force microscopy. The images were obtained in the tapping mode in air at room temperature.

3. Results and Discussion

Figure 1 shows the reflectivity profiles of the sample before and after immersion. After contacting water for a long period of time, the interlayer spacing of the film changes significantly, indicating the penetration of water into the hyhrophilic regions between the bilayers. One can infer from the multilamellar peaks a well-defined lamellar periodicity of about $d = 3.98$ nm before immersion and about $d = 4.97$ nm after immersion. It is known that the X-ray diffraction measurements can be applied not only to study the ordered assembly structure and the periodicity of the stearic acid films but also to evaluate the orientation of the hydrocarbon chain axis.[21] According to the chain length of the stearic acid molecules, it is estimated that the angle between the chain axis and the normal to the base plane is 37.2°. The periodicity of the film before immersion differs from the one calculated for two crystal modifications of stearic acid, form B and form E, in which the tilt angle of the chains is about 25°.[22,23] The difference in tilt angle can be explained as follows. The chains in low-density monolayers have a greater tilt angle than those in higher-density monolayers.[24] The stearic acid molecules in our films are packed not as tightly as those in the crystals. Therefore the tilt angle of the chains in our films is larger. To calculate the orientation of the stearic acid molecules after immersion in water, the reflectivity curve is fitted according to the method reported in refs 25 and 26. According to the difference of the electronic density between the stearic acid molecular and the water molecules, the thickness of the water layers is estimated to be 1.9 nm, and the bilayer thickness is 3.07 nm. The results are consistent with those reported in refs 27 and 28. The tilt angle of the long alkyl chains in the immersed film is about 52.1°, larger than that in the as-deposited film. It is noticeable that the Bragg peaks of the immersed film are narrower than those of the as-deposited film. The film before immersion consists of small domains, which broaden the Bragg peaks. After immersion the molecules are rearranged in the film and the change in tilt angle of the chains helps to create larger domains. Thus, the small domains fuse into larger ones so that the peaks become narrower.

To investigate the effect of the penetrated water on the structure of the film, we studied its interfacial fluctuations by the X-ray diffuse scattering. The diffuse scattering of a multilayered system is a unique transformation of the statistical height-difference correlation function defined as $g_{ij}(r) = \langle [u_i(0) - u_j(r)]^2 \rangle$, where u denotes the deviation from the mean position of the interfaces labeled by i and j.[29] The formalism to obtain the scattering intensity for different types of rough surfaces has been discussed in detail in ref 30. The type of the interfacial height-difference correlation function determines the nature of the distribution of diffusely scattered photons around the specular direction.[31] The scattering function, which is proportional to the observed intensity at point (q_x,q_z), can be expressed as[29,32]

$$S(q_x,q_z) = \sum_{m,n=0}^{N} r_m r_n^* \exp[iq_z(z_m - z_n)] \int \exp\left[-\frac{1}{2}q_z^2 g_{mn}(r)\right] \exp(-iq_x r)dr \quad (1)$$

where r_n is the Fresnel reflection coefficient[33] of layer n, and z_n denotes the position of layer n. Figures 2a and 3a show the decay of the transverse diffuse scattering intensity with q_x (in a log−log plot). For the film before immersion in water, the diffuse scattering curves obey a power law. The diffuse scattering curves change a lot after immersion in water; no obvious power law can be observed.

To confirm this observation and to trace the cause of such a difference, we have performed AFM measurements on several areas of the samples. The topographic images of scan size

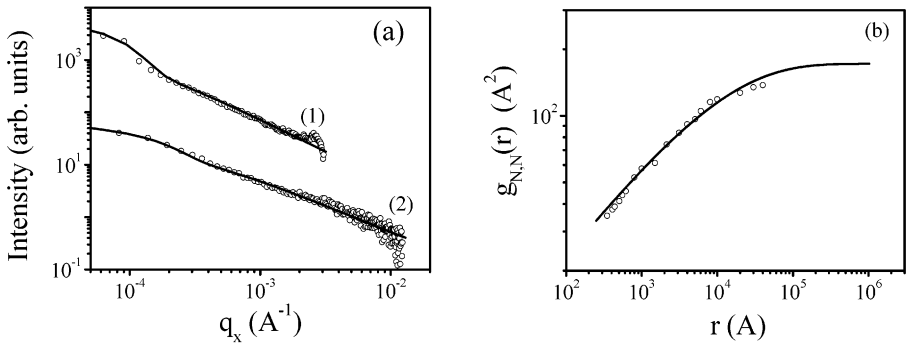

Figure 2. (a) Transverse diffuse scattering data (symbols) of the as-deposited film and the fitted curves (solid lines) using eq 2 as the correlation function. Numbers indicate the order of the Bragg peaks. (b) The height-difference correlation function $g_{N,N}(r)$ for the surface obtained from the AFM measurements (symbols) along with the fitted curve (solid lines).

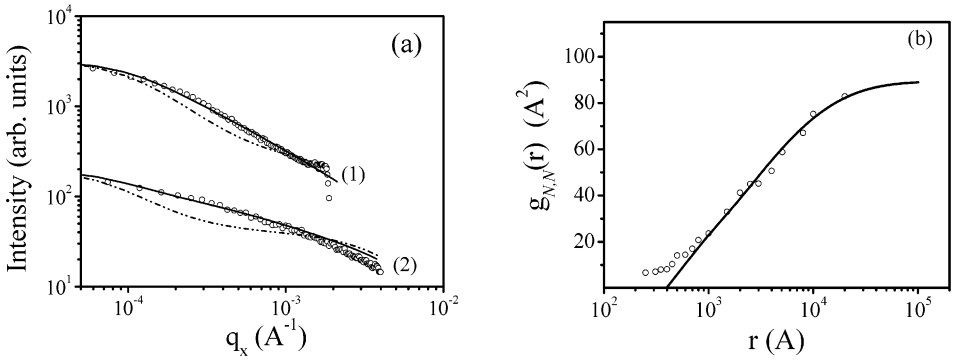

Figure 3. (a) Transverse diffuse scattering data (symbols) for the film after immersion and the fitted curves (solid lines) using eq 3 as the correlation function. Dashed lines are the calculations without taking into account the effect of the roughness fluctuations from the substrate. Numbers indicate the order of the Bragg peaks. (b) The height-difference correlation function $g_{N,N}(r)$ for the surface obtained from the AFM measurements (symbols) along with the fitted curve (solid lines).

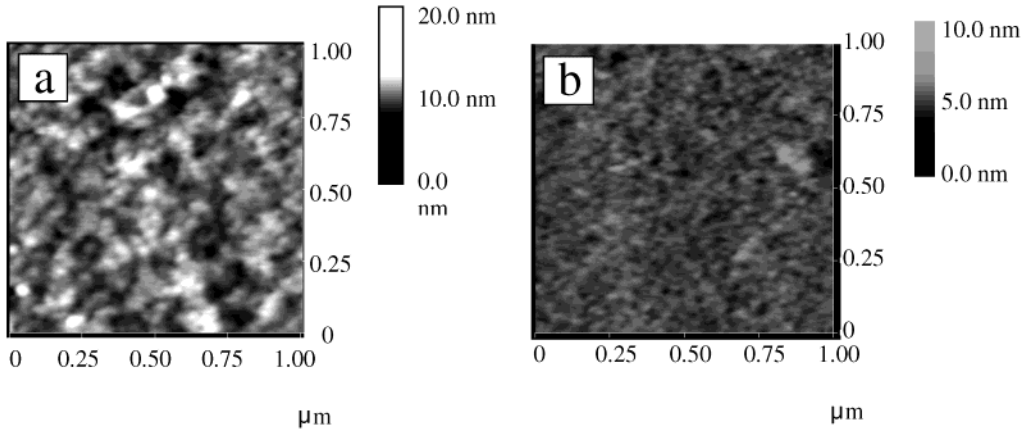

Figure 4. AFM images of scan size 1μm $\times$ 1μm for the film: (a) before immersion; (b) after immersion.

1μm$\times$1μm of the film are shown in Figure 4. With AFM, quantitative morphological information about the statistics of surfaces can be obtained. For instance, it is possible to measure the local rms roughness of a surface by performing scans of different lengths. From the scaling of this measured local roughness with scan size, it is possible to obtain the height-difference correlation function.[34] Although the AFM measurements are restricted to the top surface only, they provide information complementary to that obtained by the X-ray scattering measurements. Following ref 34, we calculated the height-difference correlation functions of the surface fluctuations for the sample before and after immersion in water, as shown in Figures 2b and 3b. The surface fluctuations of the as-deposited film is well characterized by a power law of $g(r) \propto r^{0.40}$, followed by a saturation regime at about $\xi \approx 9000$ Å. However, after immersion the surface follows a logarithmic scaling, namely, $g(r) \propto \ln(r)$.

The stearic acid film is prepared by casting the solution onto the hyhrophilic silicon surface and allowing the organic solvent to slowly evaporate. The self-affine feature of the surface hints that the film may follow the general growth dynamics of an ordinary solid.[35] In most of the investigations done so far, a specific form of the height-height correlation function for the self-affine interfaces has been used to model the X-ray diffuse scattering and the AFM data. The correlation function reads as $C_s(r) = \sigma^2 \exp[-(r/\xi)^{2h}]$.[36−38] However, our diffuse scattering curves cannot be fitted well with the above correlation function. Thus the vertical interfacial correlations must be taken into account. Vertical correlations between different interfaces i and j can be statistically described by a cross-correlation function.

Following Nitz et al.,[25,39] the correlation function is written as

$$g_{ij}(r) = \sigma_i^2 + \sigma_j^2 - 2\sigma_i\sigma_j \exp[-(r/\xi_{||})^{2h}] \exp[-|z_i - z_j|/\xi] \quad (2)$$

where σ_i is the roughness of the ith interface, h is the Hurst exponent, z_i denotes the position of interface i, and $\xi_{||}$ and ξ are the lateral and vertical correlation length, respectively.

According to the above theory, we have fitted very well the diffuse scattering curves for the as-deposited film, as shown in Figure 2a. The corresponding fitting parameters are $\sigma_1 = 4.4$ Å, $\sigma_N = 9.2$ Å, $\xi_{||} = 8000$ Å, $\xi = 3000$ Å, and $h = 0.20$. The rms roughness of the jth interface, σ_j, was determined by a linear interpolation formula from the values of the first and last layers.[25] Substituting the parameters into eq 2, one gets the height-difference correlation function for the surface of the as-deposited sample, which is in good agreement with the one deduced from the AFM measurements as shown in Figure 2b.

Both the X-ray and the AFM measurements show that the interfacial profile of the film after immersion is qualitatively different from that of the as-deposited one. It can be deduced from the AFM data that the surface fluctuations now follow the logarithmic scaling. In the past years, the logarithmic scaling of liquid surfaces,[40] polymer surfaces,[41] and Langmuir−Blodgett interfaces[42,43] has been studied extensively. It is often assumed that beyond a certain critical lateral length ξ_c, the interfaces in organic multilayered films, such as the lamellar liquid crystals,[44] behave as a correlated system, exhibiting a single logarithmic height-difference correlation for all interfaces. We have failed to use such a single correlation function to fit our data. This indicates that the interfaces are partially correlated as revealed by eq A.2 (see Appendix), which is, however, valid only for a bulk liquid crystal of infinite size. A correlation function that takes into account the boundary conditions and, at the same time, keeps the concise form of eq A.2 is written as (for the details about the deduction see Appendix)

$$g_{ij}(r) = 2\eta\left[g_{ij}^{(\infty)}(r) - \frac{1}{2}g_{ij}^{(i)}(r) - \frac{1}{2}g_{ij}^{(j)}(r)\right] + g_{ij}^{(0)}(r) \quad (3)$$

where

$$g_{ij}^{(\infty)}(r) = 2\gamma_E + Ei\left(\frac{r^2}{4\lambda|z_j - z_i|}\right) + \ln\left(\frac{r^2}{4d^2}\right)$$

$$g_{ij}^{(i)}(r) = 2\gamma_E + Ei\left(\frac{r^2}{4\lambda(z_j + z_i)}\right) + \ln\left(\frac{r^2}{8\lambda z_i}\right)$$

and

$$g_{ij}^{(0)}(r) = 2\int \frac{d^2q_{xy}}{(2\pi)^2} \exp[-\lambda(z_i + z_j)q_{xy}^2]|u(0,q_{xy})|^2[1 - \exp(iq_{xy}r)]$$

where d is the interlayer spacing, and $|u(0,q_{xy})|^2 = \int d^2r\sigma_0^2 \exp(-(r/\xi_0)^{2h}) \exp(iq_{xy}r)$ is the power spectrum of the rough surface of the substrate. $\lambda = \sqrt{K/B}$, *and* $\eta = k_BT/(8\pi\sqrt{KB})$, *where* B and K are elastic coefficients governing the compressional and bending modes of the film, respectively. σ_0 is the roughness of the substrate, $g_{ij}^{(\infty)}(r)$ corresponds to eq A.2, $g_{ij}^{(i)}(r)$ takes account of the fact that a mathematically flat surface suppresses the fluctuations, and $g_{ij}^{(0)}(r)$ represents the effect of the substrate whose correlation is assumed to be self-affine, characterized by a lateral correlation length ξ_0 and an Hurst exponent h.[29,32] The rest of the parameters are explained in the Appendix. Although eq 3 looks rather complicated, there are actually only two free fitting parameters, namely, λ and η. The parameters σ_0, ξ_0, and h for the substrate were estimated independently by fitting the diffuse scattering of the naked substrate.

We have used eq 3 to fit the diffuse scattering curves in Figure 3a by adopting the parameters of $\lambda = 60$ Å and $\eta = 13$ Å^2. The corresponding compressional and bending elastic coefficients of the film are $B = 2.11 \times 10^5$ J/m^3 and $K = 7.6 \times 10^{-12}$ J/m, which are typical for phospholipid membranes.[4,5] The parameters for the substrate as derived by fitting the diffuse scattering of the naked silicon surface are $\sigma_0 = 4.4$ Å, $\xi_0 = 800$ Å, and $h = 0.4$. The calculated curves are in good agreement with the measured ones in the range of $q_x < 2.2 \times 10^{-3}$ Å^{-1}. There exists some difference between the theoretical and the experimental data when $q_x > 2.2 \times 10^{-3}$ Å^{-1}, which is probably due to the inhomogeneous and localized static defects[4] or the collective protrusion modes.[5] This discrepancy is also reflected in the real space measurement. Symbols shown in Figure 3b are the height-difference correlation function derived from the AFM measurements. The solid line is the theoretically calculated correlation function. The agreement is very good except for $r < 600$ Å. Nevertheless, the logarithmic scaling is clear on the medium length scale.

It is worth noting that the fluctuations replicated from the substrate have to be taken into account in order to fit the diffuse scattering curves of the immersed film. The dashed lines in Figure 3a are the calculation without taking into account the effect of the roughness fluctuations from the substrate. The curves deviate from the experimental data. It indicates that the substrate has an effect on the interfacial fluctuations of the film after immersion. In addition, the infusion of water into the acid bilayers will introduce local defects, which will affect the interfacial fluctuations at a certain extent. This may account for the discrepancy between the theoretical and the experimental data when $q_x > 2.2 \times 10^{-3}$ Å^{-1}, but as has been pointed out by Sens et al.,[45] the defects do not alter the characteristics of the interfacial fluctuations very much as long as they distribute homogeneously in the film. Only the effective bending and compression moduli get renormalized.

4. Summary

The interfacial structures of the solution-cast stearic acid film before and after immersion in water were studied by the X-ray scattering combined with AFM. Theoretical fit indicates that the interfacial roughness of the as-deposited film is self-affine. After being swollen by water the film takes on a liquid crystal character. The description of the lyotropic polymorphism has since early days been developed in two opposite directions.[46] Physicochemical descriptions usually start from very diluted amphiphile solutions and follow the structuring of these solutions at increasing amphiphile concentration. A physical description begins more naturally with the addition of water to a solid crystal of an amphiphilic substance.[46] Relatively less attention has been paid to the later direction. With the invasion of the solvent, the solid structure of the film is destroyed and takes on a liquid crystal character. Although the concept has been proposed as early as in the 1960s,[12] study on the interfacial fluctuations in the process is absent. Here we have shown that X-ray scattering is a powerful tool to study the interfacial structures of the multilayered lipid membranes. The experimental results presented here indicated that the physical description can be as successful as the physicochemical one. Moreover, it helps to

have a deeper insight into the interfaces of the lipid multilayers during the intercalation of small molecules.

Acknowledgment. This work was financially supported by the National Natural Science Foundation of China (Grants 10325419 and 10274096) and by the Chinese Academy of Sciences. The authors thank Prof. L. Huang and Mr. Z. -M. Tan of the Peking University for useful discussions and for their help in the AFM measurements.

Appendix

Here we present the derivation of the correlation function, eq 3. We begin with a brief review of the interfacial fluctuation of a liquid crystal. The thermally exited interfacial fluctuations have long been the subject of liquid crystal physics.[47,48] An algebraic decay of the correlation of the interfacial fluctuation is expected from the linear smectic elasticity theory, based on the Hamiltonian

$$H = \int_V d^3r\left[\frac{1}{2}B\left(\frac{\partial u}{\partial z}\right)^2 + \frac{1}{2}K(\nabla_{xy}^2 u)^2\right] \qquad \text{(A.1)}$$

where $u(r)$ is a continuous displacement field of the membranes with respect to a perfect lattice in the local coordinate system, and B and K are elastic coefficients, governing the compressional and bending modes of the smectic phase, respectively.[49] The Hamiltonian results in the celebrated height-difference correlation function of Caille:[50,51]

$$g(r,z) = 4\eta\left[\gamma_E + \ln\left(\frac{r}{2d}\right) + \frac{1}{2}Ei\left(\frac{r^2}{4\lambda z}\right)\right] \qquad \text{(A.2)}$$

where γ_E is Euler's constant, $Ei(x) = \int_x^\infty t^{-1}\, e^{-t}dt$, $\lambda = \sqrt{K/B}$, and $\eta = k_BT/(8\pi\sqrt{KB})$.

The high-resolution X-ray scattering has demonstrated the validity of eq A.2 for the bulk lamellar phase, at least on scales larger than several nanometers.[4,5] To derive eq 3 we adopt a model that a lamellar liquid crystal is geometrically confined by a hard wall. The surface of the hard wall is assumed to be self-affine, characterized by a correlation function $C(r) = \sigma_0^2 \exp[-(r/\xi_o)^{2h}]$. The effect of the hard wall can be separated into two parts in the harmonic approximation of eq A.1. The first is simply the penetration of the surface fluctuation into the liquid crystal. Following de Gennes,[52] the Fourier spectrum of the fluctuation at a displacement z from the wall is

$$u(z,q_{xy}) = \exp(-\lambda z q_{xy}^2)u(0,q_{xy}) \qquad \text{(A.3)}$$

where $u(z,q_{xy}) = \int u(r,z)\exp(iq_{xy}r)dr$. The intercorrelation induced by the rough surface is thus

$$\langle u(z_i,0)u(z_j,r)\rangle = \int \frac{d^2q_{xy}}{(2\pi)^2}\exp[-\lambda(z_i+z_j)q_{xy}^2]|u(0,q_{xy})|^2 \exp(iq_{xy}r) \qquad \text{(A.4)}$$

where z_i denotes the position of interface i, and $|u(0,q_{xy})|^2 = \int d^2r\sigma_0^2 \exp(-(r/\xi_0)^{2h})\exp(iq_{xy}r)$. The second part takes account of the suppression of the fluctuations by a mathematically flat wall. We assume that the fluctuation of the first layer near the wall is totally suppressed. This boundary condition is automatically satisfied if the Fourier spectrum of the membrane at a distance z from the wall is written as $u(z,q_{xy}) = \int u(q_z,q_{xy})\sin(q_z z)dq_z$, where $u(q_z,q_{xy})$ is the 3D Fourier spectrum of the thermal fluctuation of a lamellar liquid crystal whose power spectrum can be written as $|u(q_z,q_{xy})|^2 = k_BT/(q_z^2 + \lambda q_{xy}^2)$ according to the equipartition theorem. The intercorrelation function is

$$\langle u(z_i,0)u(z_j,r)\rangle = \int dq_z d^2q_{xy} q_{xy}|u(q_z,q_{xy})|^2(e^{iq_z(z_i+z_j)} - e^{iq_z(z_i-z_j)})J_0(q_{xy}r) \qquad \text{(A.5)}$$

where z_i denotes the position of interface i. Equation A.5, together with eq A.4, gives the closed form for $g_{ij}(r)$ in eq 3. In most cases, the free surface of the film has much weaker effect on the interfacial fluctuations than does the hard wall. The interfacial correlation function derived here can therefore be applied directly to a stack of lipid membranes of finite thickness on a solid surface.

References and Notes

(1) Sohn, B. H.; Seo, B. H. *Chem. Mater.* **2001**, *13*, 1752.
(2) Moriguichi, I.; Hosoi, K.; Nagaoka, H.; Tanaka, I.; Teraoka, Y.; Kagawa, S. *J. Chem. Soc., Faraday Trans.* **1994**, *90*, 349.
(3) Chen, H. J.; Chai, X. D.; Wei, Q.; Jiang, Y. S.; Li, T. J. *Thin Solid Films* **1989**, *178*, 535.
(4) Salditt, T.; Munster, C.; Lu, J.; Vogel, M.; Fenzl, W.; Souvorov, A. *Phys. Rev. E* **1999**, *60*, 7285.
(5) Salditt, T.; Vogel, M.; Fenzl, W. *Phys. Rev. Lett.* **2003**, *90*, 178101.
(6) Vogel, M.; Munster, C.; Fenzl, W.; Salditt, T. *Phys. Rev. Lett.* **2000**, *84*, 390.
(7) Sharp, J. S.; Jones, R. A. L. *Phys. Rev. E* **2002**, *66*, 011801.
(8) Marshbanks, T. L.; Ahn, D. J.; Franses, E. I. *Langmuir* **1994**, *10*, 276.
(9) Girard, K. P.; Quinn, J. A.; Vanderlick, T. K. *J. Colloid Interface Sci.* **1999**, *217*, 146.
(10) Williams, R. *J. Chem. Phys.* **1963**, *39*, 384.
(11) Heilmeier, G. H.; Zanoni, J.; Barton, J. *Proc. IEEE* **1968**, *56*, 1162.
(12) Lawrence, A. S. C. *Mol. Cryst. Liq. Cryst.* **1966**, *1*, 205.
(13) Sein, A.; Van Breemen, J. F. L.; Engberts, J. B. F. N. *Langmuir* **1995,** *11*, 3565.
(14) Salditt, T. *Curr. Opin. Struct. Bio.* **2003**, *13*, 467.
(15) Basu, J. K.; Sanyal, M. K. *Phys. Rep.* **2002**, *363*, 1.
(16) Katsaras, J. *Biochem. Cell Bio.* **1995**, *73*, 209.
(17) Huang, H. W.; Liu, W.; Olah, G. A.; Wu, Y. *Prog. Surf. Sci.* **1991**, *38*, 145.
(18) Seul, M.; Eisenberger, P. *Phys. Rev. A* **1989**, *39*, 4230.
(19) Tolan, M. In *X-ray Scattering from Soft-Matter Thin Films*, Springer Tracts in Modern Physics; Hohler, G., Ed.; Springer Verlag: Karlsruhe, 1999; Vol. 148, p 113.
(20) Seul, M.; Sammon, M. J. *Thin Solid Films* **1990**, *185*, 287.
(21) Luo, X.; Zhang, Z.; Liang, Y. *Langmuir* **1994**, *10*, 3213.
(22) Sato, K.; Kobayashi, M.; Morishita, H. *J. Cryst. Growth* **1988**, *87*, 236.
(23) Kaneko, F.; Kobayashi, M.; Kitagawa, Y.; Matsuura, Y. *Acta Crystallogr.* **1990**, *C46*, 1490.
(24) Richardson, W.; Blasie, J. K. *Phys. Rev. B* **1989**, *39*, 12165.
(25) Nitz, V.; Tolan, M.; Schlomka, J. P.; Seeck, O. H.; Stettner, J.; Press, W. *Phys. Rev. B* **1996**, *54*, 5038.
(26) Tolan, M. In *X-ray Scattering from Soft-Matter Thin Films*, Springer Tracts in Modern Physics; Hohler, G., Ed.; Springer Verlag: Karlsruhe, 1999; Vol. 148, p 33.
(27) Ganguly, P.; Pal, S.; Sastry, M.; Shashikala, M. N. *Langmuir* **1995**, *11*, 1078.
(28) Ganguly, P.; Sastry, M.; Choudhury, S.; Paranjape, D. V. *Langmuir* **1997**, *13*, 6582.
(29) Sinha, S. K.; Sirota, E. B.; Garoff, S.; Stanley, H. B. *Phys. Rev. B* **1988**, *38*, 2297.
(30) Tolan, M. In *X-ray Scattering from Soft-Matter Thin Films*, Springer Tracts in Modern Physics; Hohler, G., Ed.; Springer Verlag: Karlsruhe, 1999; Vol. 148, p 118.
(31) Basu, J. K.; Sanyal, M, K.; Mukherjee, M.; Banerjee, S. *Phys. Rev. B* **2000**, *62*, 11109.
(32) Mol, E. A. L.; Shindler, J. D.; Shalaginov, A. N.; De Jeu, W. H. *Phys. Rev. E* **1996**, *54*, 536.
(33) Parratt, L. G. *Phys. Rev.* **1954**, *95*, 359.
(34) Durr, A. C.; Schreiber, F.; Ritley, K. A.; Kruppa, V.; Krug, J.; Dosch, H.; Struth, B. *Phys. Rev. Lett.* **2003**, *90*, 016104.
(35) Barabasi, A. L.; Stanley, H. E. *Fractal Concepts in Surface Growth*; Cambridge University Press: New York, 1995; p 38.
(36) Weber, W.; Lengler, B. *Phys. Rev. B* **1992**, *46*, 7953.
(37) Palasantzas, G.; Krim, J. *Phys. Rev. B* **1993**, *48*, 2873.
(38) Palasantzas, G. *Phys. Rev. B* **1993**, *48*, 14472.

(39) Ming, Z. H.; Krol, A.; Soo, Y. L.; Kao, Y. H.; Park, J. S.; Wang, K. L. *Phys. Rev. B* **1993**, *47*, 16373.
(40) Tidswell, I. M.; Rabedeau, T. A.; Pershan, P. S.; Kosowsky, S. D. *Phys. Rev. Lett.* **1991**, *66*, 2108.
(41) Tolan, M.; Seeck, O. H.; Schlomka, J.-P.; Press, W.; Wang, J.; Sinha, S. K.; Li, Z.; Rafailovich, M. H.; Sokolov, J. *Phys. Rev. Lett.* **1998**, *81*, 2731.
(42) Basu, J. K.; Sanyal, M. K. *Phys. Rev. Lett.* **1997**, *79*, 4617.
(43) Basu, J. K.; Hazra, S.; Sanyal, M. K. *Phys. Rev. Lett.* **1999**, *82*, 4675.
(44) Holyst, R. *Phys. Rev. A* **1991**, *44*, 3692.
(45) Sens, P.; Turner, M. S. *Eur. Phys. J. E* **2001**, *4*, 115.
(46) Petrov, A. G. *The Lyotropic State of Matter*; Gordon and Breach Science Publishers: Amsterdam, 1999; p 27.
(47) Safinya, C. R.; Roux, D.; Smith, G. S.; Sinha, S. K.; Dimon, P.; Clark, N. A.; Belloq, A. M. *Phys. Rev. Lett.* **1986**, *57*, 2718.
(48) Roux, D.; Safinya, C. R. *J. Phys. (Paris)* **1988**, *49*, 308.
(49) Salditt, T. *Curr. Opin. Colloid Interface Sci.* **2000**, *5*, 19.
(50) Kaganer, V. M.; Ostrovskii, B. I.; Jeu, V. H. *Phys. Rev. A* **1991**, *44*, 8158.
(51) Gunther, L.; Imry, Y.; Lajzerowicz, J. *Phys. Rev. A* **1980**, *22*, 1733.
(52) De Gennes, P. G.; Prost, J. *The Physics of Liquid Crystals*, 2nd ed., Clarendon Press: Oxford, 1993; p 338.